Vector-Valued Native Space Embedding for Adaptive State Observation

Shengyuan Niu¹, Haoran Wang¹, Heejip Moon², Andrea L'Afflitto³, Andrew Kurdila¹, Daniel Stilwell²

Abstract—This paper combines vector-valued reproducing kernel Hilbert space (vRKHS) embedding with robust adaptive observation, yielding an algorithm that is both non-parametric and robust. The main contribution of this paper lies in the ability of the proposed system to estimate the state of a plan model whose matched uncertainties are elements of an infinite-dimensional native space. The plant model considered in this paper also suffers from unmatched uncertainties. Finally, the measured output is affected by disturbances as well. Upper bounds on the state observation error are provided in an analytical form. The proposed theoretical results are applied to the problem of estimating the state of a rigid body.

I. Introduction

This paper presents an adaptive system able to estimate the state of a nonlinear plant model, whose matched nonlinearities lie in a user-defined infinite-dimensional reproducing kernel Hilbert space (RKHS – also known as native space) of vector-valued functions. This system is also designed to be robust to finite-dimensional unmatched uncertainties and disturbances in the measured output. To the authors' knowledge, this is the first work to propose an adaptive observer in a native space framework and for vector-valued matched uncertainties.

Recently, the authors commenced a systematic effort to port existing robust and adaptive control techniques from a parametric to a non-parametric framework [1, Ch. 5]. Thus far, control techniques such as control Lyapunov functions, backstepping, and model reference adaptive control (MRAC) have been ported to a native space setting [2], [3], [4], [5], [6]. Within this framework, this paper is the first to address the observation and estimation problem for multi-input multi-

This work is supported in part by the Office of Naval Research (ONR) project number N00014-24-1-2267.

output systems. A key advantage in using RKHS embedding methods lies in the ability to counter infinite-dimensional matched uncertainties, whereas existing methods rely on finite-dimensional representations of uncertainties based on a regressor vector or a similar structure. Furthermore, leveraging native space theory, it is possible to deduce tight upper bounds on the error in approximating matched uncertainties through the proposed approaches [1, Ch. 3].

The proposed theoretical results are applied to a problem of practical interest, namely, the observation of the state of a rigid body. It is worthwhile recalling that the rigid body model is typically employed to capture the dynamics of uncrewed aerial vehicles (UAVs) [7], autonomous underwater vehicles (AUVs) [8], and spacecraft [9] to name a few. In these applications, however, a characterization of the vehicle, especially of larger vehicles, and of the disturbances acting on them is usually non-trivial. Numerical methods usually require an intense effort to produce quality results and experimental methods are usually costly. Thus, estimation methods applicable to broad classes of uncertainties and that do not rely on a regressor vector or matrix to characterize uncertainties and disturbances are preferable.

This paper is structured as follows. In Section II, we summarize key properties of native spaces and recall essential results needed throughout this work. In Section IV, we present a theoretical result that captures the ideal behavior of the proposed adaptive observer. This observer involves an adaptive law evolving over the native space of functional uncertainties affecting the plant dynamics. In practice, this adaptive law is not implementable since it is infinite-dimensional. Thus, in Section V, we present finite-dimensional approximations of the results in Section IV. Section VI demonstrates the applicability of the proposed results through numerical simulations involving the translational and rotational dynamics of a rigid body. Finally, Section VII draws conclusions and outlines future work directions.

¹S. Niu, H. Wang, and A. Kurdila are with the Department of Mechanical Engineering, Virginia Tech, Blacksburg, VA 24061, USA. Email: {syniu97, haoran9, kurdila}@vt.edu.

²H. Moon and D. Stilwell are with the Bradley Department of Electrical & Computer Engineering, Virginia Tech, Blacksburg, VA 24061, USA. Email: {hmoon5, stilwell}@vt.edu.

³A. L'Afflitto is with the Grado Department of Industrial and Systems Engineering, Virginia Tech, Blacksburg, VA 24061, USA. Email: a.lafflitto@vt.edu.

II. NOTATION ON VECTOR-VALUED REPRODUCING KERNEL HILBERT SPACE

In this section, we discuss elements of RKHS theory. For a detailed account on this topic, see [1, Ch. 3]. Let $\Omega \subset \mathbb{Y} \triangleq \mathbb{R}^m$ and $\mathfrak{K} : \Omega \times \Omega \to \mathbb{R}$ be a Mercer kernel [1, Def. 3.6]. We define the scalar-valued native space

$$\mathcal{H} \triangleq \overline{\operatorname{span}\{\mathfrak{K}_y(\cdot) : y \in \mathbb{Y}\}},\tag{1}$$

where $\mathfrak{K}_y(\cdot) \triangleq \mathfrak{K}(y,\cdot)$, and the closure is taken with respect to the candidate inner product defined as

$$\langle \mathfrak{K}_{y_1}, \mathfrak{K}_{y_2} \rangle_{\mathcal{U}} \triangleq \mathfrak{K}(y_1, y_2), \text{ for any } y_1, y_2 \in \mathbb{Y}.$$
 (2)

Given \mathcal{H} , we can define the diagonal operator-valued kernel $\mathcal{K}: \mathbb{Y} \times \mathbb{Y} \to \mathcal{L}(\mathbb{U})$ so that $\mathcal{K}(y_1, y_2) \triangleq \mathfrak{K}(y_1, y_2) I_m$ for all $y_1, y_2 \in \mathbb{Y}$, where $I_m \in \mathbb{R}^{m \times m}$ denotes the identity matrix, and the vector-valued native space $\mathcal{H} \triangleq \mathcal{H}^m \triangleq \mathcal{H} \times \cdots \times \mathcal{H}$. Given $f \in \mathcal{H}$, we define the evaluation operator $E_y: \mathcal{H} \to \mathbb{U} \triangleq \mathbb{R}^m$ so that

$$E_y f = f(y) \in \mathbb{U}$$
, for all $f \in \mathbb{H}$ and for all $y \in \Omega$,
(3)

and we denote the adjoint of the evaluation operator as $E_y^{\star}: \mathcal{H} \to \mathbb{U}$. Both the evaluation operator and its adjoint are bounded and linear.

Given the set of centers $\Xi_N\subset \mathbb{Y},$ we consider the finite-dimensional RKHS

$$\mathcal{H}_N \triangleq \{ \mathcal{K}_{\xi_i}(\cdot) \alpha_i : \xi_i \in \Xi_N, \alpha_i \in \mathbb{U} \}. \tag{4}$$

to approximate the infinite-dimensional RKHS \mathcal{H} , where $\mathcal{K}_{\xi_i}(\cdot) \triangleq \mathcal{K}(\xi_i, \cdot)$. Thus, we can decompose any $f \in \mathcal{H}$ as $f = \Pi_N f + (I - \Pi_N) f$, where $\Pi_N : \mathcal{H} \to \mathcal{H}_N$ denotes the projection operator from \mathcal{H} onto \mathcal{H}_N [1, Def. 2.51]. The projection error can be bounded as $\|E_y(I - \Pi_N)f\|_{\mathbb{U}} \leq \sup_{y \in \Omega} \mathcal{P}_N(y) \|f\|_{\mathcal{H}}$ [1, Th. 3.22], where $\mathcal{P}_N(\cdot)$ denotes the power function

$$\boldsymbol{\mathcal{P}}_{N}(y) \triangleq \max_{i=1,...,m} \sqrt{\left|\mathcal{K}_{ii}(y,y) - \mathcal{K}_{N,ii}(y,y)\right|},$$

for all $y \in \mathbb{Y}$, (5)

 \mathcal{K}_{ii} denotes the element of the *i*th row and *i*th column of $\mathcal{K}(\cdot,\cdot)$, and $\mathcal{K}_N(y_1,y_2) \triangleq \mathcal{K}_{\Xi_N}(y_1)\mathbb{K}_{\Xi_N}^{-1}\mathcal{K}_{\Xi_N}(y_2)$ for all $y_1,y_2 \in \Omega$.

$$\mathcal{K}_{\Xi_N}(y) \triangleq [\mathcal{K}(y, \xi_1), \dots, \mathcal{K}(y, \xi_N)] \in \mathbb{R}^{m \times mN},$$
 (6)

and

$$\mathbb{K}_{\Xi_{N}} \triangleq \begin{bmatrix} \mathcal{K}(\xi_{1}, \xi_{1}) & \dots & \mathcal{K}(\xi_{1}, \xi_{N}) \\ \vdots & \ddots & \vdots \\ \mathcal{K}(\xi_{N}, \xi_{1}) & \dots & \mathcal{K}(\xi_{N}, \xi_{N}) \end{bmatrix} \in \mathbb{R}^{mN \times mN}$$

denotes the Grammian matrix.

III. PROBLEM STATEMENT

In this paper, we investigate the problem of estimating the state of the nonlinear system

$$\dot{x}(t) = Ax(t) + B\left(u(t) + E_{y(t)}f\right),$$

$$x(t_0) = x_0, \quad t \ge t_0, \quad \text{(8a)}$$

$$y(t) = Cx(t) + \delta(t), \tag{8b}$$

where $x:[t_0,\infty)\to\mathbb{R}^n$ denotes the *state vector*, $u:[t_0,\infty)\to\mathbb{R}^m$ denotes the *control input*, which is bounded and user-defined, $A\in\mathbb{R}^{n\times n}$, $B\in\mathbb{R}^{n\times m}$, $C\in\mathbb{R}^{m\times n}$, the pair (A,B) is controllable, the pair (A,C) is observable, the linear dynamical system

$$\dot{x}(t) = Ax(t) + Bu(t), \quad x(t_0) = x_0, \quad t \ge t_0,$$
 (9a)

$$y(t) = Cx(t), (9b)$$

is strictly positive real, the measurement error δ : $[t_0,\infty) \to \mathbb{U}$ is continuous and bounded, that is, $\|\delta(t)\| \leq \overline{\delta}$, and $f \in \mathcal{H}(\Omega,\mathbb{U})$ is unknown.

IV. A DISTRIBUTED PARAMETER SYSTEM SOLUTION

To address the proposed estimation problem, consider the *adaptive observer*

$$\dot{\hat{x}}(t) = A\hat{x}(t) + L(y(t) - C\hat{x}(t))
+ B(u(t) + E_{y(t)}\hat{f}), \quad \hat{x}(t_0) = \hat{x}_0, \quad t \ge t_0,
(10)$$

where $L \in \mathbb{R}^{n \times m}$ chosen such that $A_e \triangleq A - LC$ is Hurwitz, the adaptive gain $\hat{f}: [t_0, \infty) \times \Omega \to \mathcal{H}$ denotes the solution of the adaptive law

$$\frac{\partial}{\partial t}\hat{f}(t,\cdot) = \mu_{\text{step}}\left(e(t), E_0\right) \Gamma_f E_{y(t)}^*(y - C\hat{x}),$$
$$\hat{f}(t_0, \cdot) = f_0, \quad t \ge t_0, \quad (11)$$

the adaptive rate matrix $\Gamma_f \in \mathbb{R}^{m \times m}$ is symmetric and positive-definite,

$$\mu_{\text{step}}(e, E_0) \triangleq \begin{cases} 1, & \text{if } e \notin \mathring{\mathcal{B}}_{E_0}(0_n), \\ 0, & \text{otherwise,} \end{cases}$$
(12)

denotes the *step function*, the closed ball $\overline{\mathcal{B}}_{E_0}(0_n)$ centered at 0_n and of radius

$$E_0 \triangleq \frac{\overline{\delta} \| L^{\mathrm{T}} P \|}{\epsilon \lambda_{\min}(P) + \lambda_{\min}(W^{\mathrm{T}} W)}$$
 (13)

denotes the *dead-zone*, and the symmetric positive-definite matrix $P \in \mathbb{R}^{n \times n}$, the matrix $W \in \mathbb{R}^{p \times n}$, and the scalar $\epsilon > 0$ verify the Lur'e equations

$$A_e^{\mathrm{T}}P + PA_e = -W^{\mathrm{T}}W - \epsilon P, \tag{14a}$$

$$PB = C^{\mathrm{T}}. (14b)$$

The effectiveness of the observer (10) and the adaptive law (11) is captured by the following result.

Theorem 1. Consider the nonlinear dynamics (8) and the observer (10). If the dynamical system given by (8) and (10) has a unique solution $(\hat{x}, \tilde{f}) \in \mathbb{R}^n \times C^1([t_0, \infty), \mathcal{H})$ for every initial condition, then, there exists $T \geq t_0$ such that $e(t) \in \overline{\mathcal{B}}_{E_0}(0_n)$ for all $t \geq T$.

Proof. Let $e(t) \triangleq x(t) - \hat{x}(t)$, $t \geq t_0$, denote the *state* observation error. It follows from (8) and (10) that the state observation error dynamics are given by

$$\dot{e}(t) = A_e e(t) + BE_{y(t)}\tilde{f} - L\delta(t),$$

$$e(t_0) = x_0 - \hat{x}_0, \quad t \ge t_0, \quad (15)$$

where $\tilde{f} \triangleq f - \hat{f}$. Thus, consider the *Lyapunov function candidate*

$$V(e, \tilde{f}) = \langle e, Pe \rangle_{\mathbb{R}^n} + \left\langle \tilde{f}, \Gamma_f^{-1} \tilde{f} \right\rangle_{\mathcal{H}},$$

$$(e, \tilde{f}) \in \mathbb{R}^n \times \mathcal{H}.$$
(16)

Taking the time derivative of (16) along the trajectories of (15) and (10), it holds that

$$\dot{V}(t,e,\tilde{f}) = \langle \dot{e}(t), Pe \rangle_{\mathbb{R}^{n}} + \langle e, P\dot{e}(t) \rangle_{\mathbb{R}^{n}} + 2 \left\langle \partial_{t} \tilde{f}(t,\cdot), \Gamma_{f}^{-1} \tilde{f} \right\rangle_{\mathcal{H}}$$

$$= \left\langle A_{e}e + B(E_{y(t)}\tilde{f}) - L\delta(t), Pe \right\rangle_{\mathbb{R}^{n}}$$

$$+ \left\langle e, PA_{e}e + PB(E_{y(t)}\tilde{f}) - PL\delta(t) \right\rangle_{\mathbb{R}^{n}}$$

$$- 2 \left\langle \partial_{t} \tilde{f}(t,\cdot), \Gamma_{f}^{-1} \tilde{f} \right\rangle_{\mathcal{H}}$$

$$= \left\langle e, (A_{e}^{T} P + PA_{e}) e \right\rangle_{\mathbb{R}^{n}}$$

$$- 2 \left\langle e, PL\delta(t) \right\rangle_{\mathbb{R}^{n}} + 2 \left\langle \tilde{f}, E_{y(t)}^{*} B^{T} Pe \right\rangle_{\mathcal{H}}$$

$$- 2 \left\langle \partial_{t} \tilde{f}(t,\cdot), \Gamma_{f}^{-1} \tilde{f} \right\rangle_{\mathcal{H}}$$

$$= -e^{T} W^{T} We - \epsilon e^{T} Pe - 2 \left\langle e, PL\delta(t) \right\rangle_{\mathbb{R}^{n}}$$

$$+ 2 \left(\left\langle \tilde{f}, E_{y(t)}^{*} Ce - \Gamma_{f}^{-1} (\Gamma_{f} E_{y}^{*} (y - C\hat{x}))) \right\rangle_{\mathcal{H}}$$

$$= -e^{T} W^{T} We - \epsilon e^{T} Pe + 2\bar{\delta} \|L^{T} P\| \|e\|,$$

$$(t, e, \tilde{f}) \in [t_{0}, \infty) \times \mathbb{R}^{n} \times \mathcal{H}. (17)$$

Now, with the adaptive law (10), if $e \notin \overline{\mathcal{B}}_{E_0}$, then $\dot{V}(t,e,\tilde{f}) < 0$; if $e \in \partial \mathcal{B}_{E_0}$, then $\dot{V}(t,e,\tilde{f}) = 0$; and if $e \in \mathring{\mathcal{B}}_{E_0}$, then the sign of $\dot{V}(t,e,\tilde{f})$ is undefined. Therefore, if $e(t_0) \notin \overline{\mathcal{B}}_{E_0}$, then there exists $t_1 > t_0$ such that $e(t) \in \partial \mathcal{B}_{E_0}$. The time t_1 can be estimated by noting that $\dot{V}(t,e,\tilde{f}) \leq -C$, where

$$C \triangleq \sup \left\{ -\dot{V}(t, e, \tilde{f}) : \\ (t, e, \tilde{f}) \in [t_0, \infty) \times \left(\overline{\mathcal{B}}_{\|e(t_0)\|} \setminus \mathring{\mathcal{B}}_{E_0} \right) \times \mathcal{H} \right\}$$

is positive, and, hence,

$$t_1 \le t_0 - C^{-1}V(e(t_0), \tilde{f}(t_0)).$$
 (18)

Since $\dot{V}(t,e(t),\tilde{f}(t))$ is not sign definite for all $t>t_1$ such that $e(t)\in \mathring{\mathcal{B}}_{E_0}$ and $\dot{V}(t,e(t),\tilde{f}(t))\leq 0$ for all $t\geq t_1$ such that $e(t)\in \partial \mathcal{B}_{E_0}$, there exist time sequences $\{t_{2k+1}\}_{k=0}^M$ and $\{t_{2k}\}_{k=1}^M$ with $M\in \overline{N}\cup \{\infty\}$ such that $e(t)\in \partial \mathcal{B}_{E_0}$ for all $t\in [t_{2k+1},t_{2k+2}]$ and for all $k\in \{0,\ldots,M\}$, and $e(t)\in \mathring{\mathcal{B}}_{E_0}$ for all $t\in (t_{2k},t_{2k+1})$ and for all $k\in \{1,\ldots,M\}$. Therefore, for all $t\geq t_1$, the trajectory tracking error $e(\cdot)$ is bounded to reside within $\overline{\mathcal{B}}_{E_0}$ and $\|\tilde{f}(t)\|\leq \|\tilde{f}(t_1)\|$ for all $t\geq t_1$. The case whereby $e(t_0)\in \mathring{\mathcal{B}}_{E_0}$ can be deduced following similar arguments and is omitted for brevity.

Theorem 1 provided a sufficient condition for the adaptive observer (10) and the adaptive law (11) to estimate the plant state. At steady state, the observation error is commensurate with the known upper bound $\overline{\delta}$ on the measurement error $\delta(\cdot)$. Ideally, if $\delta(t) \equiv 0_m$ for all $t \geq t_0$, then Theorem 1 guarantees asymptotic convergence of the observation error to zero.

Theorem 1 is based on the assumption of the uniqueness of the solutions of (8) and (10) for all initial conditions. Sufficient conditions to verify this assumption can be deduced by proceeding as in the proof of Theorem 5.4 of [1], and are omitted for brevity.

V. IMPLEMENTABLE ADAPTIVE LAWS

The adaptive law (11) is a distributed parameter system (DPS), and, hence, is no implementable in practice. In this section, we present finite-dimensional approximations of (11). However, as discussed in [1, Ch. 5] in the context of adaptive control systems design over native spaces, finite-dimensional approximations of DPSs induce error terms that must be accounted for by a robustification of the adaptive mechanism. In this section, we discuss a smooth dead-zone modification of the adaptive estimation system presented in Section IV. The classical dead-zone modification of adaptive laws [10] is discontinuous and, hence, breaks the canonical assumptions of Lipschitz continuity of the tracking error dynamics. Furthermore, in practice, the dead-zone modification of MRAC may induce chattering. For these reasons, a smooth implementation of the dead-zone modification is considered.

A. Smoothed Dead-Zone Modification

Consider the finite-dimensional adaptive law

$$\dot{\hat{f}}_{N}(t) = \sigma_{0}(\|e\|_{\mathbb{Y}}(t), d, \varepsilon)\Gamma_{f}\Pi_{N}\mathcal{K}_{y(t)}(y(t) - C\hat{x}(t)),$$

$$\hat{f}_{N}(t_{0}) = f_{0}, \quad t \geq t_{0},$$
(19)

where the *dead-zone* width d is such that

$$d > d_N$$

$$\triangleq \frac{2\|C\|_2(\sup_{y\in\mathbb{Y}} \mathcal{P}_N(y) \|(I - \Pi_N)f\|_{\mathcal{H}} + \|PL\|_2\overline{\delta})}{\lambda_{\min}(W^{\mathrm{T}}W + \epsilon P)},$$
(20)

where $\lambda_{\min}(\cdot)$ denotes the eigenvalue of its argument with the smallest real part. The function $\sigma_0: \mathbb{R} \times \mathbb{R} \times \mathbb{R} \to \mathbb{R}$ is a Δ -admissible dead-zone in its first argument.

Definition 1 ([11]). Let $\Delta > 0$. A continuously differentiable function $\sigma_{\Delta} : \mathbb{R}^+ \to \mathbb{R}$ is an Δ -admissible dead-zone if

- $0 \le \sigma_{\Delta}$ and $\sigma_{\Delta}(x) = 0$ for all $x \in [0, \Delta]$,
- $0 \le \dot{\sigma}_{\Delta}$ and $\sigma_{\Delta}(x) = 0$ for all $x \in [0, \Delta]$,
- $\dot{\sigma}_{\Delta}(\cdot)$ is locally Lipschitz,

An example of an admissible dead-zone is given by

$$\sigma_0(\|e\|_{\mathbb{V}},d,\varepsilon)$$

$$\triangleq \begin{cases} 0, & \text{if } \|e\|_{\mathbb{Y}} \leq d, \\ \frac{(\|e\|_{\mathbb{Y}} - d)^2}{2\varepsilon}, & \text{if } \|e\|_{\mathbb{Y}} \in [d, d + \varepsilon], \\ \|e\|_{\mathbb{Y}} - (d + \varepsilon), & \text{if } \|e\|_{\mathbb{Y}} \geq d + \varepsilon, \end{cases}$$
(21)

where the dead-zone width d>0 and the buffer zone width $\varepsilon>0$ are user-defined. The first derivative of this function is given by

$$\dot{\sigma}_{0}(\|e\|_{\mathbb{Y}}, d, \varepsilon) = \begin{cases} 0, & \text{if } \|e\|_{\mathbb{Y}} \leq d, \\ \frac{\|e\|_{\mathbb{Y}} - d}{\varepsilon}, & \text{if } \|e\|_{\mathbb{Y}} \in [d, d + \varepsilon], \\ 1, & \text{if } \|e\|_{\mathbb{Y}} \geq d + \varepsilon, \end{cases}$$

$$(22)$$

which is Lipschitz continuous.

Theorem 2. Consider the plant model (8), the adaptive observer 10, and the adaptive law (19). If the dead-zone d width satisfies the condition in (20), then there exists $T \in [t_0, \infty)$ such that $\|e(t)\|_{\mathbb{Y}} \triangleq \|x(t) - \hat{x}(t)\|_{\mathbb{Y}} \leq d$ for all t > T.

Proof: The proof follows by proceeding as in the proof of Theorem 5.5 in [1], and is omitted for brevity. \Box

The ultimate bound postulated by Theorem 2 correlates the observation error to the ability of capturing matched uncertainties through the native space approximation \mathcal{H}_N . Indeed, it follows from (20) that the ultimate bound on the observation error varies with the ability of \mathcal{H}_N to capture \mathcal{H} , which is measured by the power function (5). As discussed in [1, Ch. 3], the denser the distribution of kernel centers Ξ_N , the smaller the power function, and, hence, the smaller the width of the dead-zone the user can enforce. However, the larger the number of centers, the larger the computational cost. Indeed, the dimension of the Grammian matrix grows with the square of kernel centers, that is, it grows proportionally to N^2 . The ultimate bound on the estimation error also grows with $\|(I - \Pi_N)f\|_{\mathcal{H}}$,

which is an alternative measure of the ability of \mathcal{H}_N to approximate \mathcal{H} . Finally, as expected, the observation error grows with the upper bound $\bar{\delta}$ on the observation disturbance.

B. Coordinate Implementation

To implement the finite-dimensional adaptive law (19), we let

$$\hat{f}_N(t,\cdot) = \sum_{j=1}^N \mathcal{K}_{\xi_j}(\cdot)\hat{\alpha}_j, \quad t \ge t_0, \tag{23}$$

where $\Xi_N \triangleq \{\xi_1, \dots, \xi_N\}$ denotes the set of centers. Thus, we observe that, for all $t \in [t_0, \infty)$,

$$\sum_{j=1}^{N} \mathcal{K}_{\xi_{j}}(\cdot) \dot{\hat{\alpha}}_{j}(t)$$

$$= \Gamma_{f} \Pi_{N} \mathcal{K}_{y(t)}(\cdot) (y(t) - C\hat{x}(t))$$

$$= \Gamma_{f} \left\langle \mathcal{K}_{\xi_{i}}(\cdot), \Pi_{N} \mathcal{K}_{y(t)}(\cdot) \right\rangle_{\mathcal{H}} (y(t) - C\hat{x}(t))$$

$$= \Gamma_{f} \left\langle \Pi_{N} \mathcal{K}_{\xi_{i}}(\cdot), \mathcal{K}_{y(t)}(\cdot) \right\rangle_{\mathcal{H}} (y(t) - C\hat{x}(t))$$

$$= \Gamma_{f} \left\langle \mathcal{K}_{\xi_{i}}(\cdot), \mathcal{K}_{y(t)}(\cdot) \right\rangle_{\mathcal{H}} (y(t) - C\hat{x}(t))$$

$$= \Gamma_{f} \mathcal{K}_{\xi_{i}}(y(t)) (y(t) - C\hat{x}(t)), \tag{24}$$

and

$$\sum_{j=1}^{N} \mathcal{K}_{\xi_{j}}(\cdot) \dot{\hat{\alpha}}_{j}(t) = \sum_{j=1}^{N} \left\langle \mathcal{K}_{\xi_{i}}(\cdot), \mathcal{K}_{\xi_{j}}(\cdot) \right\rangle_{\mathcal{H}} \dot{\hat{\alpha}}_{j}(t)$$

$$= \sum_{j=1}^{N} \mathcal{K}(\xi_{i}, \xi_{j}) \dot{\hat{\alpha}}_{j}(t)$$

$$= \sum_{j=1}^{N} \mathbb{K}_{\Xi_{N}, ij} \dot{\hat{\alpha}}_{j}(t). \tag{25}$$

Thus, it follows from (24) and (25) that

$$\dot{\hat{\alpha}}(t) = \Gamma_f \mathbb{K}_{\Xi_N}^{-1} \mathcal{K}_{\Xi_N}(y(t))(y(t) - C\hat{x}(t)),$$

$$\hat{\alpha}(t_0) = \alpha_0, \quad t \ge t_0, \quad (26)$$

where \mathbb{K}_{Ξ_N} is given by (7), and $\mathcal{K}_{\Xi_N}(\cdot)$ is given by (6).

VI. NUMERICAL EXAMPLE

In this section, we apply the proposed theoretical framework to the problem of estimating the state of a rigid body. First, we will address the problem of estimating its position from the measured translational velocity. Thus, we will address the problem of estimating its angular position.

A. Estimating the Translational Position

The translational dynamics of a rigid body are captured by (8a) with $x(t) = \left[r^{\mathrm{T}}(t), v^{\mathrm{T}}(t)\right]^{\mathrm{T}}$, $t \geq t_0$, $r: [t_0, \infty) \to \mathbb{R}^3$ denoting the position of the body's center of mass in an inertial reference frame \mathbb{I} , $v: [t_0, \infty) \to \mathbb{R}^3$ denoting the velocity of the

body's center of mass in \mathbb{I} , $A = \begin{bmatrix} 0_{3\times3} & I_3 \\ 0_{3\times3} & 0_{3\times3} \end{bmatrix}$ $B = \begin{bmatrix} 0_{3\times3} & m^{-1}I_3 \end{bmatrix}^{\mathrm{T}}, m > 0$ denoting the mass of the body, $f \in \mathcal{H}$ denoting some force acting on the body, and $\xi:[t_0,\infty)\to\mathbb{R}^3$ capturing some force that does not lie in the user-defined native space \mathcal{H} . In problems of practical interest, the translational position is deduced from the translational velocity, which is measured by fusing data from inertial measurement units (IMUs) and other sources of information, such as cameras. Thus, in general (8b) captures the measured output with $C = [0_{3\times3}, I_3]$. Furthermore, it is worthwhile noting how, in general, external forces acting on the body are functions of its velocity and, hence, a representation of the matched uncertainty in (8a) as $E_{y(t)}f$, where $y(t) = v(t) + \delta(t)$, is adequate; fluid dynamic forces, for instance, verify this assumption. The measurement error $\delta(\cdot)$ captures the unavoidable noise of the sensors.

B. Estimating the Angular Position

The rotational equations of motion of a rigid body are given by

$$\begin{split} \dot{\eta}(t) &= J(\eta(t))\omega(t), \quad \eta(t_0) = \eta_0, \quad t \geq t_0, \quad \text{(27a)} \\ \dot{\omega}(t) &= I^{-1} \left[u(t) - \omega^\times(t)I\omega(t) + E_{y(t)}f \right] + \xi(t), \\ \omega(t_0) &= \omega_0, \quad \text{(27b)} \end{split}$$

where $\eta(t) \triangleq [\phi(t), \theta(t), \psi(t)]^{\mathrm{T}} \in \mathcal{D}$ denotes the AUV attitude through a 3-2-1 sequence of implicit Euler angles [12, Ch. 1] of the body reference frame $\mathbb{J}(\cdot)$ relative to $\mathbb{J}, \mathcal{D} \triangleq [0, 2\pi) \times \left(-\frac{\pi}{2}, \frac{\pi}{2}\right) \times [0, 2\pi), \omega : [t_0, \infty) \to \mathbb{R}^3$ denotes the angular velocity, $(\cdot)^{\times} : \mathbb{R}^3 \to \mathrm{so}(3)$ denotes the cross-product operator, $I \in \mathbb{R}^3$ denotes the symmetric, positive-definite inertia matrix, $f \in \mathcal{H}$ denotes moments of external forces acting on the body, and $\xi : [t_0, \infty) \to \mathbb{R}^3$ captures moments of forces that can not be modeled as elements of a native space.

It is well-known that (27) can not be reduced to the same form as (8a). However, (27b) is in the same form as (8a) with $x(t) = \omega(t)$, $t \ge t_0$, $A = 0_{3\times 3}$, and $B = I^{-1}$. In problems of practical interest, it is common practice to directly measure the angular velocity using IMUs so that $C = I_3$. Thus, we apply the proposed framework to deduce $\omega(\cdot)$ despite uncertainties due to f, $\xi(\cdot)$, and $\delta(\cdot)$.

C. Numerical Results

To implement the proposed results, we consider the Sobolev-Matérn kernel $\mathcal{K}(\xi, x) = \sigma(\|\xi - x\|)I_3$, where

$$\sigma(r) = \frac{2\pi^{d/2}}{\Gamma(k)} K_{k-d/2} (r/2)^{k-d/2}, \quad r \ge 0$$
 (28)

for $d, k \in \mathbb{N}$. Additional details of this kernel function can be found in [1, Ch. 3]. The adaptive rate for both examples is set $\Gamma_f = 1$.

To estimate position translational of the rigid body, let m4 kg and $-K_{P,r}(x(t) - x_r(t)) + B^{\dagger}\dot{x}_r(t)$ u(t)= $\begin{bmatrix} I_{3\times3} & I_{3\times3} \end{bmatrix}$ and $x_r(t) \triangleq$ where $K_{P,r}$ $\begin{bmatrix} \sin(t) & \cos(t) & \sin(2t) & \cos(t) & -\sin(t) & 2\cos(2t) \end{bmatrix}^{\mathrm{T}}$ denotes the user-defined reference trajectory. We set the deadzone d = 0.01 and buffer zone $\varepsilon = 0.01$. The nonlinear external force f was chosen as $f = \left[\cos(x_4^2), \sin(x_5^2) + \sin(x_4), \cos(x_6) + \sin(x_5)\right]$ and the disturbance $\delta(t) = 0.008(\sin(0.5t) + \cos(0.5t))$. The basis centers for this example are placed on a three-dimensional lattice in the velocity space with three centers on each dimension, totaling 27 basis centers. The range of the 3D lattice is [-1,1] for all three dimensions.

To estimate the attitude of the rigid body, the dead-zone was chosen to be d=0.1 and the buffer zone was $\varepsilon=0.01$. The inertia matrix considered in this example is $I=\mathrm{diag}[0.2,15,15]~\mathrm{kg}~\mathrm{m}^2$. The control input is set $u(t)=-K_{P,\omega}(\omega(t)-\omega_r(t))+\dot{\omega}_r(t)$, where $K_{P,\omega}=10\cdot I_3$. The reference trajectory is chosen as $\omega_r(t)=[0.1\cos(0.1t),0.1\sin(0.1t),0.1\tanh(0.1t)]^\mathrm{T},$ $t\geq t_0$. In addition to the Coriolis term $\omega^\times(t)I\omega(t),$ $t\geq t_0$, the matched uncertainty in the rotational dynamics was chosen to be $f=-0.001\|\omega\|\omega$. The measured output disturbance is chosen as $\delta(t)=0.05\sin(5t),$ $t\geq t_0$. The basis centers for this example are placed in the space of angular velocities in the same manner as the transitional dynamics example. The range of the 3D lattice is [-0.1,0.1] for all three dimensions.

Figures 1–3 capture the main results of the proposed simulations. Figure 2 shows a sizable error in the pitch angle and the roll angle estimation. This error is the result of a large deadzone, which is designed to cover both $\delta(t)$ and the estimation error. This behavior highlights the limitation of the smoothed deadzone. To prevent parameter drift, the estimation performance must be sacrificed.

VII. CONCLUSION

This paper presented an adaptive observation framework for uncertain nonlinear systems by embedding unknown dynamics into a vector-valued reproducing kernel Hilbert space. The method extends adaptive estimation to both infinite- and finite-dimensional adaptive laws, incorporating a smoothed dead-zone modification to ensure boundedness and robustness. Numerical results concerning the dynamics of rigid bodies demonstrated the applicability of the proposed theory.

Future work directions are multi-fold. Of great interest will be the addition of non-deterministic matched,

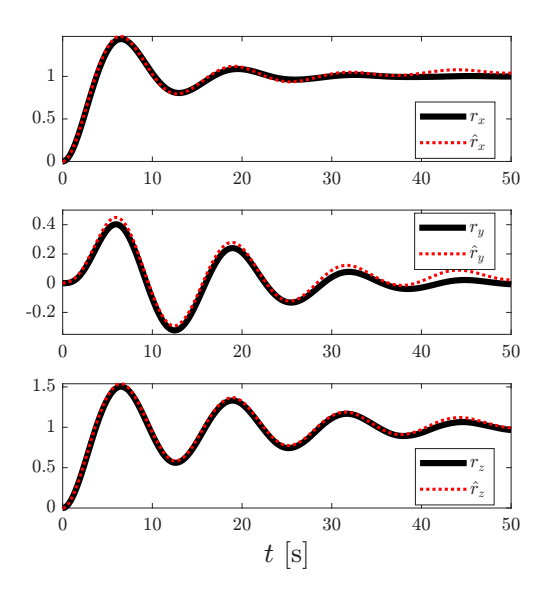


Fig. 1: Actual translational position and the estimated translational position as functions of time

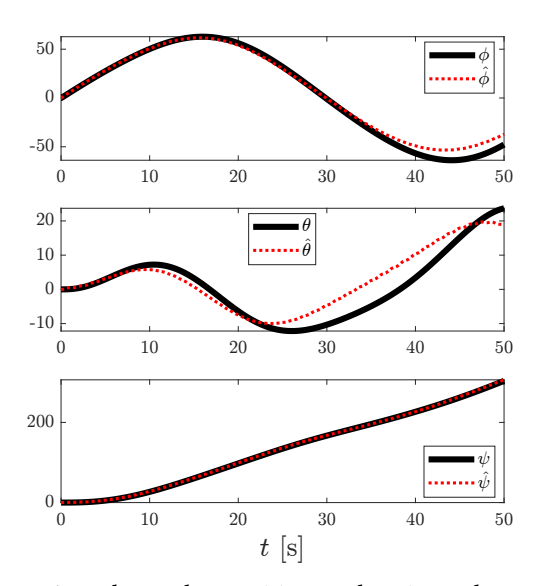


Fig. 2: Actual angular position and estimated angular position as functions of time

unmatched, and measurement disturbances. Additional areas of interest concern merging adaptive control and estimation techniques over native spaces for an integrated output-feedback MRAC framework.

References

- A. J. Kurdila, A. L'Afflitto, and J. A. Burns, *Data-Driven, Non-parametric, Adaptive Control Theory.* London, UK: Springer, 2025.
- [2] S. T. Paruchuri, J. Guo, and A. Kurdila, "Reproducing kernel hilbert space embedding for adaptive estimation of nonlinearities in piezoelectric systems," *Nonlinear Dynamics*, vol. 101, no. 2, pp. 1397–1415, 2020.

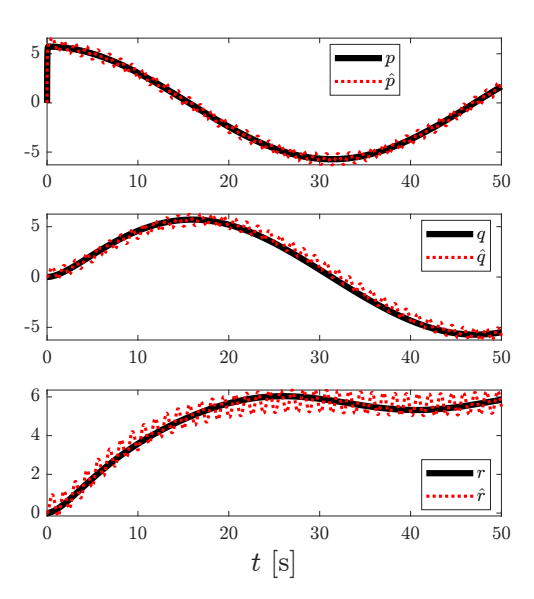


Fig. 3: Actual angular rate and estimated angular rate as functions of time

- [3] J. Guo, M. E. Kepler, S. Tej Paruchuri, H. Wang, A. J. Kurdila, and D. J. Stilwell, "Adaptive estimation of external fields in reproducing kernel hilbert spaces," *International Journal of Adaptive* Control and Signal Processing, vol. 36, no. 8, pp. 1931–1957, 2022.
- [4] J. Guo, S. T. Paruchuri, and A. J. Kurdila, "Approximations of the reproducing kernel hilbert space (rkhs) embedding method over manifolds," in 2020 59th IEEE Conference on Decision and Control (CDC). IEEE, 2020, pp. 1596–1601.
- [5] ——, "Partial persistence of excitation in rkhs embedded adaptive estimation," *IEEE Transactions on Automatic Control*, vol. 68, no. 10, pp. 5850–5861, 2022.
- [6] J. A. Burns, J. Guo, A. J. Kurdila, S. T. Paruchuri, and H. Wang, "Error bounds for native space embedding observers with operator-valued kernels," in 2023 American Control Conference (ACC). IEEE, 2023, pp. 4796–4801.
- [7] J. A. Marshall, W. Sun, and A. L'Afflitto, "A survey of guidance, navigation, and control systems for autonomous multi-rotor small unmanned aerial systems," *Annual Reviews in Control*, vol. 52, pp. 390–427, 2021.
- [8] T. Njaka, S. Brizzolara, and D. J. Stilwell, "Guide for cfd-informed auv maneuvering models," Society of Naval Architects and Marine Engineers, 2022.
- [9] J. Sullivan, S. Grimberg, and S. D'Amico, "Comprehensive survey and assessment of spacecraft relative motion dynamics models," *Journal of Guidance, Control, and Dynamics*, vol. 40, no. 8, pp. 1837–1859, 2017.
- [10] B. Peterson and K. Narendra, "Bounded error adaptive control," IEEE Transactions on Automatic Control, vol. 27, no. 6, pp. 1161– 1168, 1982.
- [11] N. M. Boffi, S. Tu, and J.-J. E. Slotine, "Nonparametric adaptive control and prediction: Theory and randomized algorithms," *Journal of Machine Learning Research*, vol. 23, no. 281, pp. 1–46, 2022
- [12] A. L'Afflitto, A Mathematical Perspective on Flight Dynamics and Control. London, UK: Springer, 2017, doi:10.1007/978-3-319-47467-0.